

Fabrication of Creep Tubing from the US and NIFS Heats of V-4Cr-4Ti

A.F. Rowcliffe, D.T. Hoelzer (Oak Ridge National Laboratory), W.R. Johnson (RSME Services, San Diego), C.Young (Century Tubes Inc, San Diego).

OBJECTIVE

Utilize commercial-scale processing to fabricate small-diameter, thin-wall tubing from plate stock of V-4Cr-4Ti for both the US program heat no. 832665 and the NIFS-HEAT-2 and produce sufficient tubing to meet programmatic needs for investigating creep behavior in both lithium and vacuum environments and for carrying out irradiation creep measurements.

SUMMARY

The first batch of commercially-fabricated creep tubing from the US program heat of V-4Cr-4Ti has been used for the on-going program of creep measurements in vacuum and Li environments and also for irradiation creep measurements both in ATR and in HFIR. This tubing (Batch A) had a fairly high frequency of surface cracking both at the ID and OD surfaces and both carbon and oxygen concentrations increased significantly during tube processing. Recently a second tubing campaign was undertaken (Batch B) to produce sufficient tubing to continue creep studies within both the US and Japanese programs. To overcome the shortcomings of Batch A tubing, modifications were made to the procedure including changes to the drawing schedule to reduce drawing stresses and changes to the cleaning procedures to reduce carbon pick-up. During the processing of Batch A, intermediate anneals at 1000°C were carried out under vacuum conditions in the 10^{-4} torr range. For Batch B, vacuum conditions of $< 2 \times 10^{-5}$ torr were specified and a different vendor selected.

In spite of these improvements, the rate of oxygen pick-up was higher during Batch B processing by a factor of 3-4. Because of the dependence of oxygen concentration on the surface area; volume ratio, the oxygen content of the tubing doubled during the final 2 anneals to reach 1745 wppm for the US heat and 1645 wppm for the NIFS heat. To reduce oxygen concentrations to more acceptable levels, a double heat treatment in liquid Li at 800°C and 1000°C was devised which lowered oxygen levels to below 750 wppm and simultaneously produced a uniform grain size distribution with 12-15 grains across the tubing wall for both heats. A sufficient number of creep tubes were prepared in this way for the RB-17J irradiation experiment in HFIR. Further experiments were carried out to determine the origins of the enhanced pick-up of oxygen in Batch B. Processing variables investigated included a) differences in furnace geometry, leak rate and vacuum measurement between the two vendors, b) differences in gettering procedure and c) differences in the rate of attack during the acid cleaning procedure.

Our preliminary conclusions are that although the above processing variables have some significance, the primary cause of the enhanced rate of oxygen pick-up is related to changes in the mechanism of oxidation of the V-4Cr-4Ti alloy with changes in the partial pressure of oxygen during the annealing treatment. The evidence suggests that under poor vacuum conditions (Batch A) the uptake of oxygen is slowed by the formation of a temporarily protective oxide film. Under improved vacuum conditions (Batch B) the protective oxide film does not form and the oxygen concentration increase more rapidly. It is probable that during Batch A processing conditions, a major fraction of the oxygen in the form of a visible oxide film, was removed each time the tubing was acid cleaned. Further investigation of these factors is proceeding with the object of defining a set of conditions under which a further batch of tubing could be fabricated with minimal oxygen pick-up.

PROGRESS AND STATUS

Introduction

The pressurized tube creep specimen measures 25.4mm long with a 4.57mm outside diameter and a wall thickness of 0.25mm. In 1995, Argonne National Laboratory coordinated a campaign to fabricate ~6

meters of tubing from the US program heat No.832665 with Century Tubes Inc. of San Diego as the primary sub-contractor [1]. This effort met with mixed success with a large fraction of the tubing developing cracks on both the inside and outside surfaces. These cracks were frequently linked together through the wall thickness via a band of severe macroscopic deformation. Since they were long enough to be visible to the naked eye, it was possible to select relatively sound segments of tubing to prepare a sufficient number of creep specimens to meet short term needs. This tubing was used for an initial series of testing both in vacuum and in lithium environments [2] and was also used to develop irradiation creep data in experiments conducted in the ATR [1] and in the HFIR [3]. However it was not possible to eliminate all defects by visual inspection, and it has been suggested that defects in the tube wall could be responsible for inconsistencies in the measured strains to failure. Thus an important goal for this tubing campaign was the elimination of surface cracking. In addition to the cracking problems it was also found that the levels of interstitials increased significantly during processing with carbon increasing from 80 to 300 wppm, oxygen increasing from 310 to 700 wppm and nitrogen increasing slightly from 85 to 95 wppm. The increase in oxygen was of particular concern since creep rate is sensitive to oxygen concentrations in this range and in general the analysis of creep behavior is complicated by the removal of oxygen during testing in Li and the pick-up of oxygen during ultra-high vacuum creep testing. The goal adopted for the new creep tube fabrication campaign was to maintain oxygen levels in the 300-400 wppm range so that at least the initial oxygen level would be similar to that for the other mechanical property specimens fabricated from plate-stock of V-4Cr-4Ti.

Two small heats of V-4Cr-4Ti with low levels of interstitials have been produced in Japan under the direction of the National Institute for Fusion Sciences (NIFS). A small quantity of creep tubing was prepared from the NIFS-HEAT-2 material using a three-directional rolling process [4]. Less severe problems were encountered with interstitial pick-up and the development of surface defects. Based upon the experience gained from processing the US heat into tubing (Batch A) and the experience gained from processing the NIFS heat, a new procedure was developed which was designed to minimize interstitial pick-up, improve initial surface quality and reduce the probability of surface cracking by lowering stress levels in the final drawing stages. These changes and the rationale behind them were detailed in the previous semi-annual progress report [5] which also described the status of the Batch B, US and NIFS tubing after 7 drawing and 8 annealing cycles. The present report documents the remaining steps to the completion of the campaign and describes the results of intermittent interstitial analyses and metallographic examination and an assessment of the quality of the final creep tubing.

BATCH B REVISED PROCEDURE

The complete drawing and annealing schedule for the Batch B tubing from both the US and NIFS heats is shown in Table 1; the drawing schedule for the earlier Batch A tubing from the US heat is shown in Table 2. To overcome the problems of surface cracking encountered with Batch A and to minimize oxygen pick-up, a number of changes were made to the Batch A procedure [4], which may be summarized as follows;

- a) The intermediate heat treatments for Batch A were carried out by a commercial vendor (Certified Metalcraft) using a tube furnace with a reported vacuum in the 10^{-4} torr. range. For Batch B a minimum vacuum of 2×10^{-5} torr was specified and the heat treatments carried out by a different vendor (Bodycote) using a large volume oven furnace capable of operating in the 10^{-6} torr range.
- b) It was conjectured that the cracking problems encountered in Batch A resulted from a combination of high surface oxygen levels picked up during the annealing cycle and high stresses imposed by the large reductions in area, ($> 40\%$ per cycle), specified in the drawing schedule. For Batch B therefore it was specified that the reduction in area (R/A) per cycle should not exceed $\sim 30\%$. for the last 6 drawing cycles.
- c) A more rigorous cleaning operation involving successive treatments in Alconox, acetone and alcohol was introduced as a more effective mean of removing die lubricant prior to annealing. A less aggressive acid cleaning procedure was introduced consisting of a 30sec treatment with $20\% \text{HNO}_3 + 10\% \text{HF} + 70\% \text{H}_2\text{O}$ compared with the Batch A treatment of 5min with $20\% \text{HNO}_3 + 20\% \text{HF} + 60\% \text{H}_2\text{O}$.

The twin requirements of reducing drawing stresses and reducing the rate of oxygen pick-up are somewhat in conflict since reducing the reductions per draw means an increase in the number of draw cycles and hence an increase in the number of anneals. Thus in Batch A the final size was achieved with a total of 10 anneals at 1000°C for 1 hour whereas the modified procedure for Batch B necessitated a total of 13 anneals. However it was reasoned that the additional 3 hours at temperature would not result in higher oxygen levels since the specified vacuum was an order of magnitude better than that used during the processing of Batch A.

Table 1. Drawing schedule for Batch B tubing of US and NIFS heats.

Cycle No.	OD (ins)	ID (ins)	Wall (ins)	RA/Cycle %	Anneal No.
Tube blank	1.010	0.626	0.192		1
1	0.940	0.600	0.170	17.3	2
2	0.818	0.542	0.138	30.4	3
3	0.723	0.499	0.112	31.3	4
4	0.588	0.420	0.084	44.4	5
5	0.495	0.375	0.060	44.7	6
6	0.395	0.299	0.048	42.5	7
7	0.318	0.240	0.039	39.0	8
8	0.288	0.224	0.032	29.2	9
9	0.262	0.212	0.025	29.0	10
10	0.246	0.208	0.019	30.2	11
11	0.229	0.199	0.015	31.0	12
12	0.203	0.179	0.012	32.0	13
13	0.188	0.168	0.010	21.0	
Sizing	0.180	0.160	0.010	5.5	
				Final 26.5%	

Table 2. Drawing schedule for Batch A tubing of US heat.

Cycle No.	OD (ins)	ID (ins)	Wall (ins)	RA/Cycle %	Anneal No.
Tube blank	1.100	0.770	0.165		1
1	0.981	0.750	0.177	40.6	2
2	0.920	0.750	0.085	33.3	3
3	0.863	0.750	0.057	41.1	4
4	0.830	0.750	0.040	34.4	5
5	0.755	0.700	0.029	37.6	6
6	0.688	0.650	0.020	41.5	7
7	0.606	0.580	0.015	41.1	8
8	0.520	0.500	0.010	45.9	9
9	0.288	0.264	0.012	40.0	10
10	0.178	0.157	0.011	45.4	

CHARACTERIZATION OF BATCH B TUBING

INTERSTITIAL PICK-UP

Archive samples for chemical analysis and metallography were removed after each draw and after each vacuum anneal. During this study several anomalously high values for both oxygen and carbon were

encountered and it was shown that these were due to contamination during sectioning and cleaning to prepare the analysis sample. Using careful cutting and cleaning procedures and multiple samples it was determined that the overall uncertainty in determining oxygen was of the order of +/- 15%. The interstitial analysis data for both heats is shown in Table 3.

Table 3. Chemical analysis (wppm) for Batch B tubing

Anneal No.	Wall (mm)	U.S. Heat			NIFS Heat		
		C	O	N	C	O	N
BLANK	4.87	119	331	88	59	130	156
1	4.87	134	346	93	63	152	132
2	4.32						
3	3.50						
4	2.85						
5	2.13	169	403	92	85	219	140
6	1.52	119	511	94			
7	1.22	155	494	101	90	378	148
8	0.99	179	637				
9	0.81						
10	0.64				223	741	210
11	0.48	264	994	133	253	879	206
12	0.38						
13	0.31	457	1745	170	390	1675	211

In the previous semi-annual report [4], data were available up to the eighth anneal for the US heat and the seventh anneal for the NIFS heat. At this stage the oxygen content had approximately doubled for both heats and with 5-6 more stages to be completed, these increases in oxygen were of concern. Accordingly, one half of the tubing from both heats was put on hold following the eighth anneal. After carefully checking the cleaning and Ta tenting procedures and ensuring that the vacuum was maintained at better than 2×10^{-5} torr while at temperature, processing to final size was completed on the other half of both heats.

In spite of these precautions, the rate of pick-up of oxygen accelerated rapidly in the final cycles. During the final two anneals, the oxygen content of both heats approximately doubled to reach 1745 wppm for the US heat and 1675 wppm for the NIFS heat. Significant increases also occurred in both the nitrogen and carbon concentrations of both heats. Thus in spite of the efforts to improve the fabrication procedures, the final oxygen content of the Batch B tubing was more than double that of the earlier Batch A tubing; carbon and nitrogen levels were also elevated above those for Batch A (C- 300wppm; N- 95wppm) but not as dramatically.

For a given set of vacuum conditions, exposure time and temperature, the quantity of oxygen adsorbed depends on specimen geometry and is proportional to the surface area:volume ratio. The surface area:volume ratio (SAV) of the tubing is plotted for each annealing cycle in Figs.1 and 2. (For a cylindrical tube the SAV is equal to $2/t$ where t is the wall thickness). The oxygen analysis data is also plotted for each stage. A curve having approximately the same shape as the SAV curve has been drawn through the oxygen analysis data. The rapid acceleration in the oxygen concentration reflects the rapid increase in SAV during the final 4-5 stages of the drawing schedule.

SURFACE DEFECTS

At the end of the fifth drawing cycle several longitudinal surface defects were observed on the OD of the US heat tubing which at this stage had a wall thickness of 1.5mm. The original plate material was characterized by a banded microstructure with arrays of Ti(CON) particles associated with regions of finer

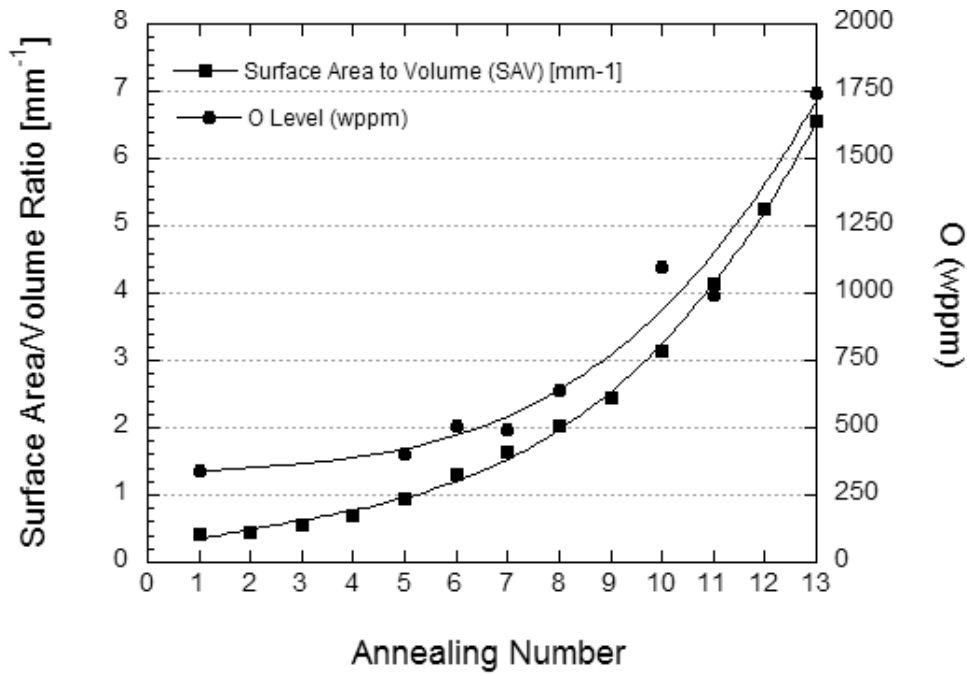


Figure 1. SAV ratio and O concentration versus annealing cycle for Batch B (U.S. Heat).

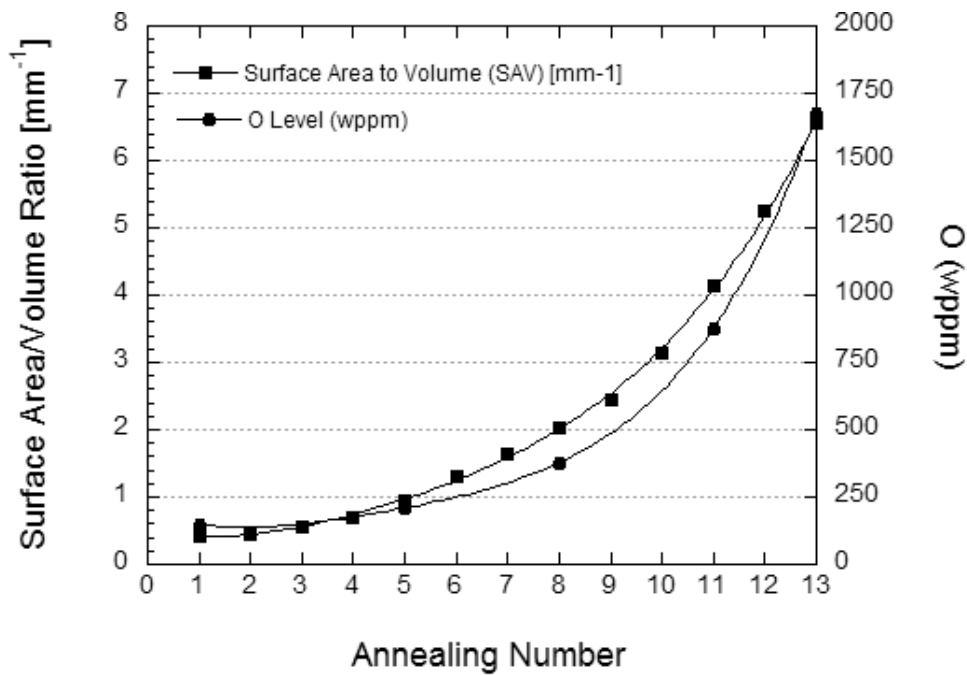


Figure 2. SAV ratio and O concentration versus annealing cycle for Batch B tubing (NIFS Heat).

gains where grain growth was impeded by the particles.[5]. At the outset it was recognized that the development of the cracks which penetrated from both surfaces in the Batch A tubing [4] was possibly related to regions of severe microstructural inhomogeneity in the original plate. A mechanism based on the rotation of bands of particles and their intersection with the surface during successive drawing stages

has been suggested to explain the cracking observed in the NIFS tubing prepared in Japan [6]. Accordingly, during the processing of Batch B one of the LT surfaces of the original plate was designated as the top surface (zero degrees) and the corresponding position was tracked during tube drawing so that the appearance of surface defects could be related to the orientation of the bands in the original plate.

At the end of the fifth drawing cycle several longitudinal surface defects were detected visually on the OD of the tubing from the US heat. The defects occurred parallel to the drawing direction at a location of 90 degrees to the original top surface of the plate. Each defect appeared to be a shallow region approximately 1-2 mm long which had separated from the tube surface. Following the sixth draw cycle the tube from the US heat was cut into 2 sections with the region containing the defects confined to a localized region of one tube (Tube A, 177 cm long) while the other tube (TubeA1, 127 cm long) appeared to be defect-free. The development of these defects at a stage where very little oxygen pick-up had occurred (total oxygen 403wppm), and their localization in one section of the tubing strongly suggests that they are related to a macroscopic inhomogeneity in the original cold-rolled plate rather than developing from a loss of near-surface ductility due to oxygen pick-up. Defects of this type were not observed in the NIFS heat tubing at this stage of the drawing.

As noted above, one half of the tubing was put on hold because of concerns regarding the extent of oxygen pick-up. Tube A1 was held back and processing continued with Tube A, a portion of which contained the visible defects. After the eighth draw cycle tube A was again cut into two sections and the section containing the visible defects was designated Tube A2. After further sub-division into sections, A2 and A4, section A2 which contained multiple visible defects developed extensive longitudinal cracks during the eleventh draw cycle and processing was discontinued. The remaining sections continued through to the final draw to 4.57 mm OD and 0.254 mm wall thickness. For the US heat, three of the final tubes (A, AA, and A3, total length ~385 cm), contained very few visible surface defects. The fourth tube (A4, total length ~200 cm) contained approximately 30 visible defects irregularly spaced along one side of the tube.

Thus Batch B at this stage, delivered sufficient length of sound tubing for ~150 creep tubes with a further 200 cm (Tube A4) which could be used by judiciously avoiding regions containing visible defects. Similarly with the NIFS heat, ~100 cm of tubing (Tube B1) was put on hold after the eighth anneal because of concerns with oxygen pick-up. The other half of the tubing (Tube B) was processed satisfactorily without any signs of surface defects until during the final draw (No.13) when one section (B2, 138 cm long), developed longitudinal cracks which linked together and produced significant splitting; processing of this section was discontinued. A total length of ~370 cm of final tubing virtually free from visible defects was produced from the NIFS heat during Batch B processing.

MICROSTRUCTURE

During the early stages of processing the recrystallized microstructures were uniform across the wall thickness and consisted of well-developed equi-axed grains; Fig. 3 shows the microstructure following the fifth anneal. The microstructure of the NIFS heat was uniform with an average grain size of ~50 microns. The US heat contained a much higher fraction of small grains (5- 10 microns) with an overall average grain size of ~ 28 microns. These grain size differences are probably related to the differences in oxygen concentration, which at this stage is 400 wppm for the US heat and 220 wppm for the NIFS heat, and also differences in the number density and distribution of Ti (CON) particles in the starting plate materials. As noted previously [4], there was clear evidence at this stage that the original bands of Ti(CON) particles become strongly curved, particularly near the OD wall, as the grains rotate to accommodate the deformation as the material is drawn through the die.

As the drawing schedule progressed, the recrystallized microstructures reflected the increasing concentration of interstitials, particularly oxygen. A near surface zone developed which etched very differently and was characterized by very fine irregularly shaped grains. After the tenth anneal the oxygen concentrations had increased to ~950 and ~741 wppm in the US and NIFS heats respectively and the

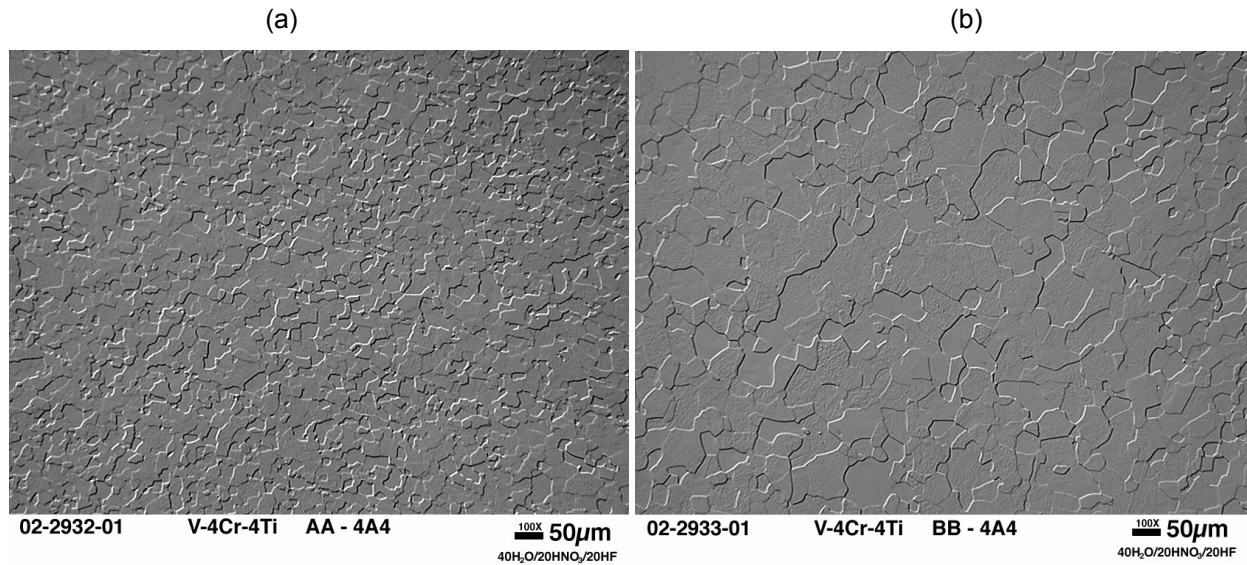


Figure 3. Optical micrographs of the Batch B tubes of the (a) US Heat and (b) NIFS Heat after the fifth anneal.

surface zones were 40-50 microns in depth Fig. 4. In some areas, primarily in the US heat, small cracks penetrated from the surface and were arrested at the edge of the zone. At this stage the average grain sizes in the central areas of the wall were ~62 and ~29 microns for the US and NIFS heats respectively. During the eleventh anneal the oxygen concentrations increase to ~1150 wppm (US) and ~880 wppm (NIFS) and the surface-affected layers increased to 60-80 microns deep at the OD surface and 40-50 microns deep at the ID. The interior microstructures however were still similar to the microstructures after the fifth anneal, with the NIFS heat still having a factor of ~2 larger grain size. After the thirteenth anneal at Bodycote, the tubes were given a draw of 25.6% R/A to reach final size. During the thirteenth anneal, oxygen concentrations increased to 1770 wppm and 1675 wppm in the US and NIFS heats respectively. The microstructures resulting from a subsequent anneal at ORNL of 2 hours at 1000°C in a vacuum of 10^{-6} torr are shown in Fig. 5. The tubing from both heats are similar with very irregular inhomogeneous grain structures suggesting extensive grain boundary pinning during recrystallization, and surface zones characterized by very fine grains extending 60-70 microns in from the OD surface and about 30-40 microns in from the ID. In spite of the very high oxygen concentrations, there was no generalized surface cracking.

To obtain more detailed information on the nature of the oxidation process and in particular the partitioning of oxygen between the matrix and the Ti(CON) particles, tubing cross-sections were examined using a Scanning-Auger system (PHI 680). Details of the surface zone in the US heat tubing following the tenth anneal (950 wppm oxygen) are shown in the scanning images of Fig. 6. Within the zone, grain growth is severely limited by the high number density of Ti(CON) particles with sizes in the range 0.1-0.5 microns. A detailed analysis of the composition of the particles, the partitioning of oxygen between the matrix and the particles and a discussion of the mechanisms of oxidation and will be reported later. However the preliminary findings indicate that a process of internal oxidation occurs with oxygen combining with Ti to form new particles of the globular form of Ti(CON) with possibly growth of the pre-existing Ti(CON)s also occurring. The number density of particles increases towards the surfaces, with most of the oxygen being associated with the Ti(CON) particles. There are no significant difference between the oxygen concentration in the matrix regions located near the center of the tube wall and the matrix regions near the surfaces.

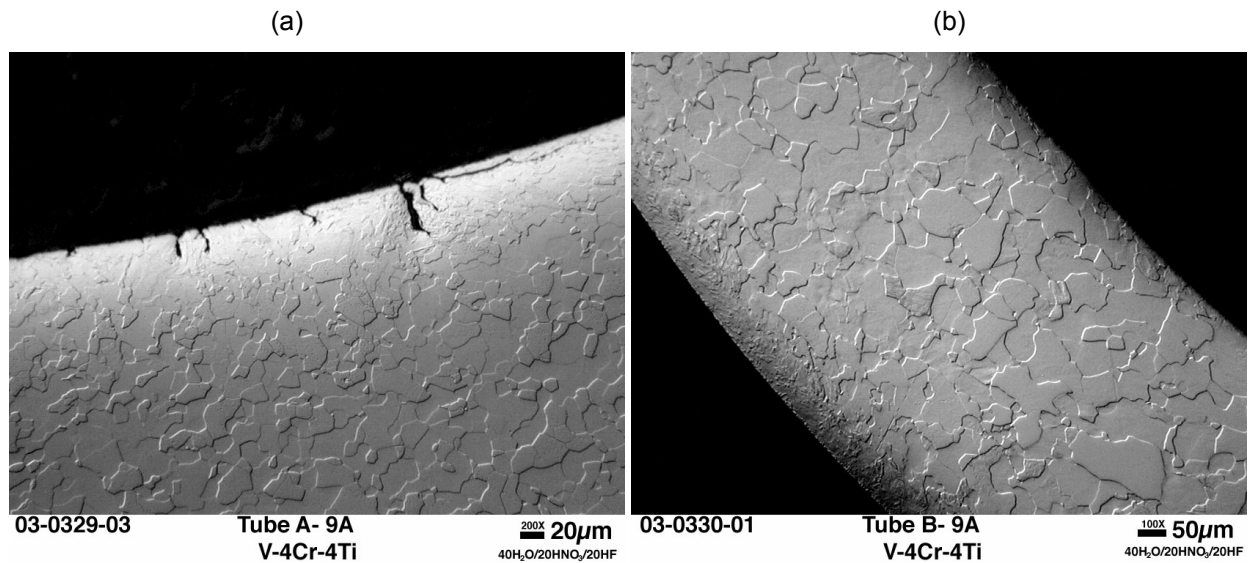


Figure 4. Optical micrographs of the Batch B tubes of the (a) US Heat and (b) NIFS Heat after the tenth anneal.

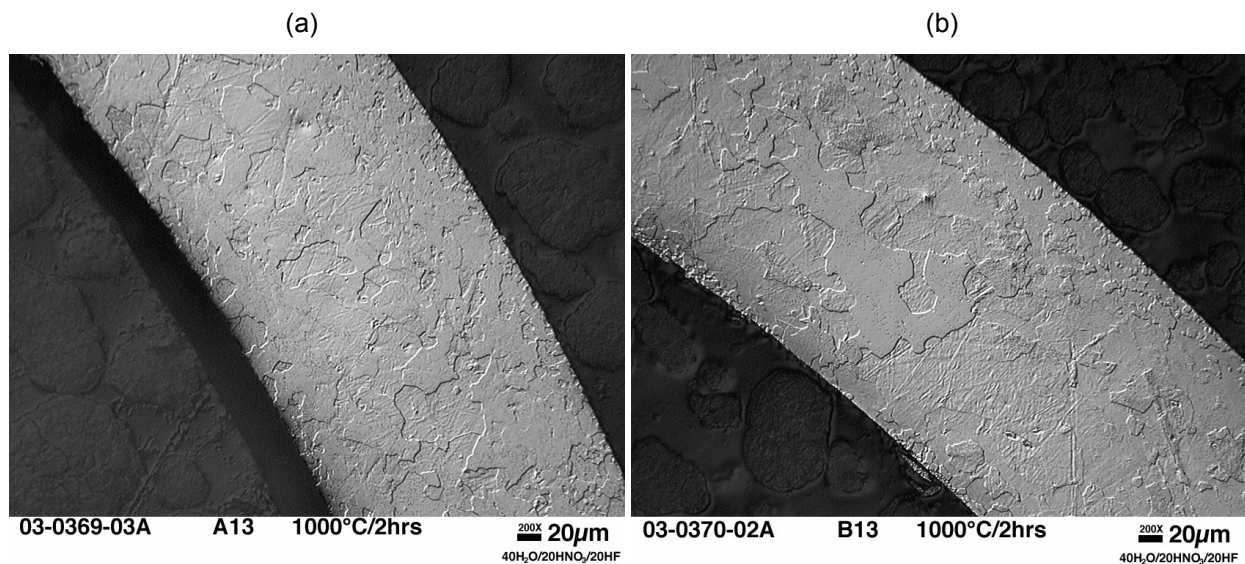


Figure 5. Optical micrographs of the Batch B tubes of the (a) US Heat and (b) NIFS Heat after annealing in vacuum for 2 hr at 1000°C.

OXYGEN REMOVAL

The high overall oxygen content and inhomogeneous grain structure of the finished tubing made it unacceptable for the fabrication of irradiation creep specimens and it was decided to reduce the oxygen content by exposing non-pressurized creep specimens to Li, at 800°C -1000°C, in a closed retort system. Previous experience with creep testing the Batch A tubing in molten Li at 800°C had shown that the kinetics of oxygen transport were sufficiently high to make this a viable approach to lowering the oxygen levels of the Batch B tubing down to the 700 wppm level of the Batch A tubing. A series of different heat

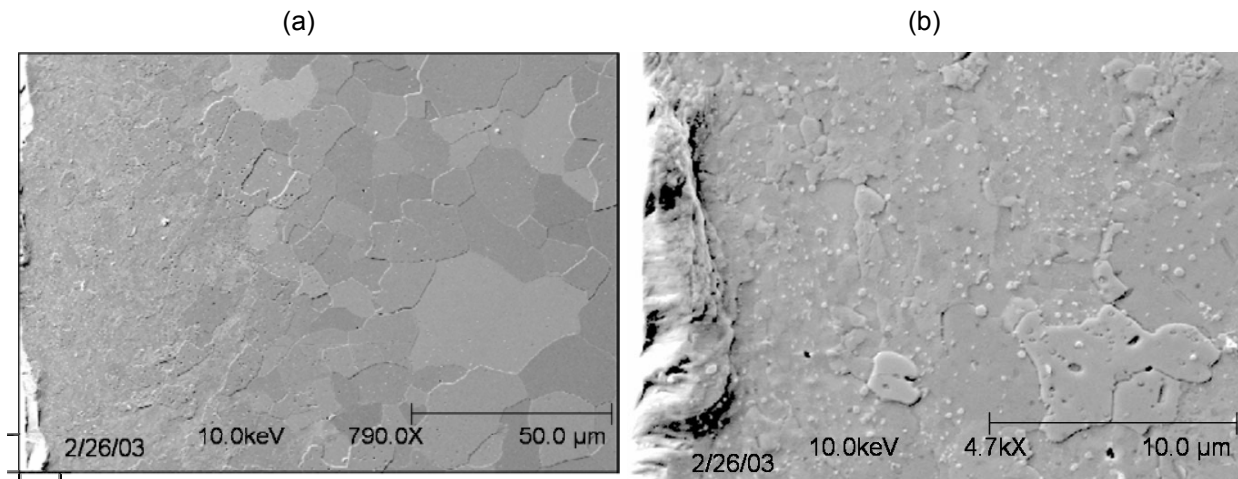


Figure 6. SEM micrographs showing (a) the changes in grain size from surface to the interior of the tube wall and (b) the increase in number density of TiCON particles near the surge region of the Batch B tube (US Heat) after the tenth anneal.

treatments were carried out to accomplish the twin goals of lowering the oxygen concentration and developing a homogeneous recrystallized microstructure with a minimum of 10-12 grains across the tube wall. A summary of the interstitial concentrations following various heat treatments is shown in Fig. 7.

During the initial treatment of one week in Li at 800°C, the oxygen concentration of the US heat tubing was reduced from 1745 wppm to 1060 wppm, confirming the viability of this approach to achieving acceptable oxygen levels. At this temperature, recrystallization does not occur and recovery may be strongly impeded by the high density of particles and elevated matrix oxygen levels, Fig. 8. The hardness decreased from the as-drawn value of 213 DPH down to 164 DPH, substantially higher than a fully recrystallized value of ~ 140 DPH.

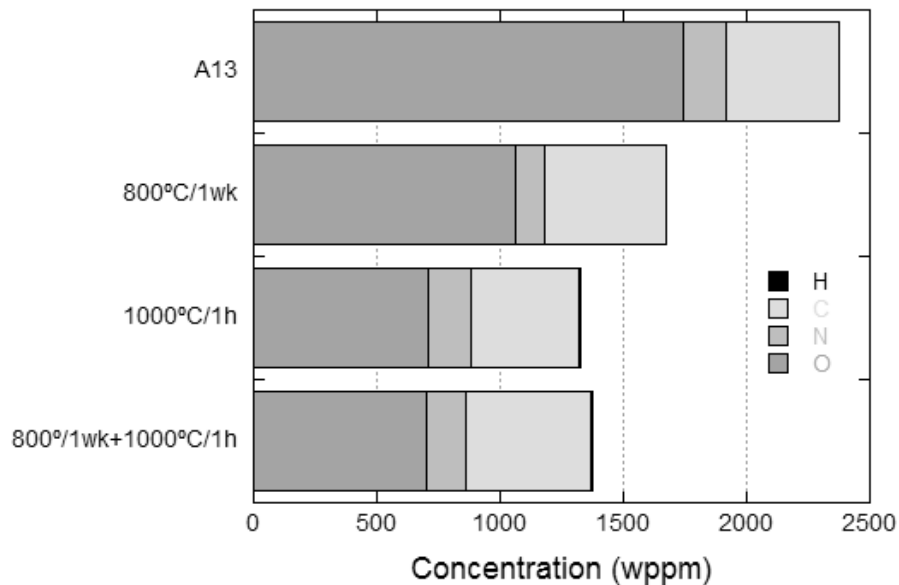


Figure 7. Interstitial concentrations measured in the Batch B tube (US Heat) following various conditions of exposure to molten Li.

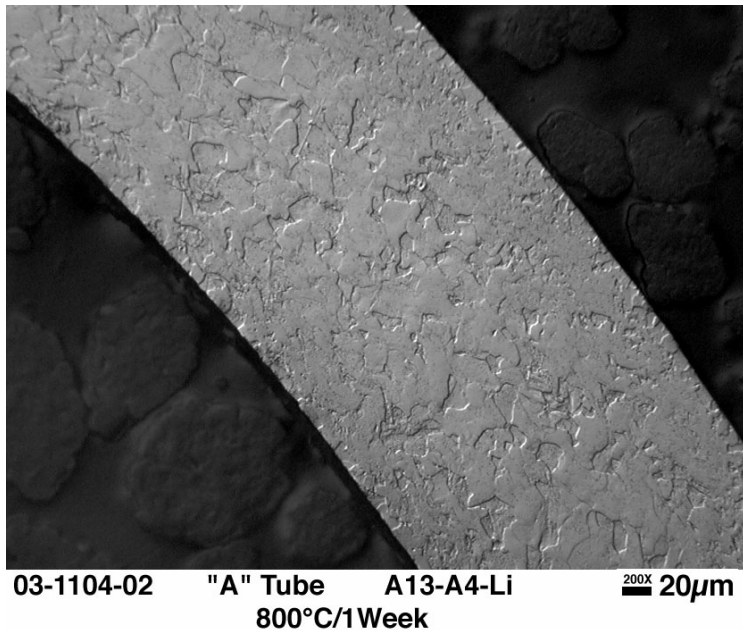


Figure 8. Optical micrograph of the Batch B tube(US Heat) after exposing in molten Li for 1 week at 800°C.

The Li temperature was increased to 1000°C to induce full recrystallization and it was found that a one hour treatment at 1000°C reduced oxygen to acceptable levels for both heats, (710 wppm for the US heat and 572 wppm for the NIFS heat). Although recrystallization did occur, the grain size distribution was not uniform across the tube wall, Fig. 9. In the US heat, a zone of smaller grains extended some 50-60 microns in from the OD surface and 15-25 microns in from the ID surface. A possible explanation for this microstructure is that the nucleation and growth of new grains is strongly influenced by the size and

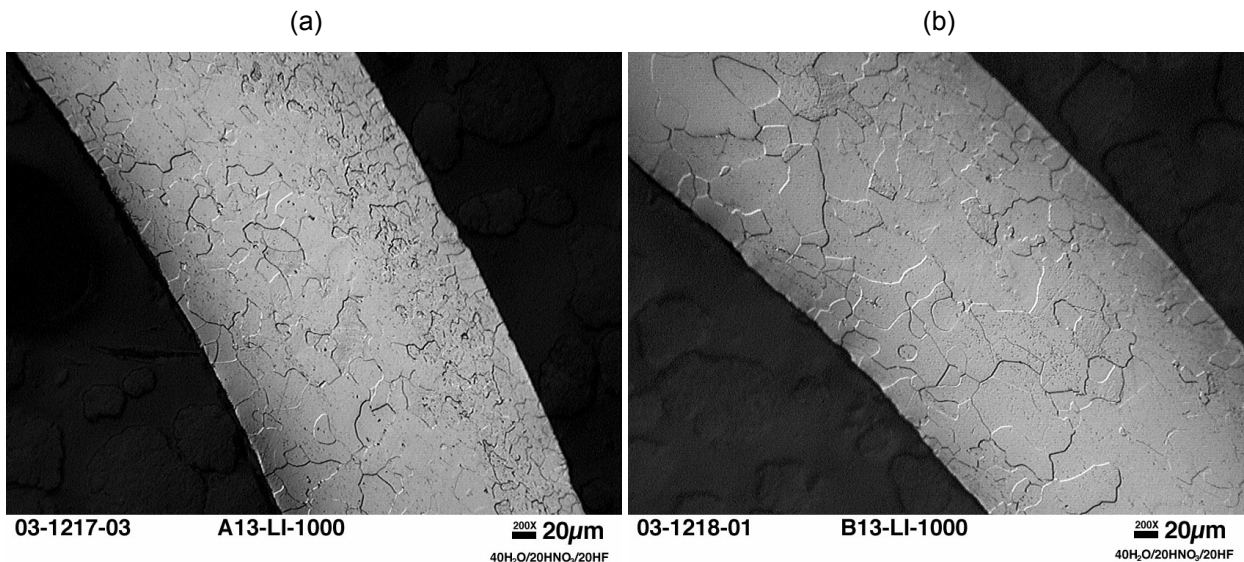


Figure 9. Optical micrographs of the Batch B tubes of the (a) US Heat and (b) NIFS Heat after exposing in molten Li for 1 hr at 1000°C.

number density of Ti(CON)s and that nucleation of new grains occurred rapidly before significant dissolution of the Ti(CON)s had take place. Based on these observations it was decided to combine the two Li exposure treatments and to allow Ti(CON) dissolution and oxygen transfer to the Li to occur at 800°C before raising the temperature and recrystallizing at 1000°C.

The double heat treatment of one week at 800°C followed by one hour at 1000°C lowered the oxygen concentrations to 700 wppm for the US heat, (analysis for the NIFS heat was not available at the time of writing but is expected to be of the same order). The levels of carbon and nitrogen were virtually unchanged by the exposures to Li. For both heats the double Li treatment resulted in a fully recrystallized microstructure with a fairly uniform grain distribution and approximately 12-15 grains across the tube wall. Apparently a sufficiently high level of stored energy is retained during the 800°C exposure to drive recrystallization in the subsequent treatment at 1000°C. The dissolution of the Ti(CON) particles occurs to such an extent that grain growth is fairly uniform across the tube wall and the surface zone of fine grains

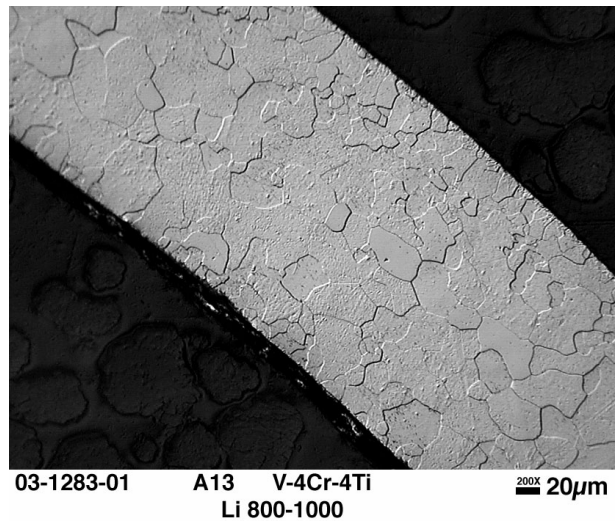


Figure 10. Optical micrograph of the Batch B tube (US Heat) after exposing to molten Li for 1 week at 800°C followed by 1 hr at 1000°C.

is eliminated, Fig. 10. A detailed description of the final preparation of pressurized creep tubes including final dimensions, fill pressures, and profilometry measurements will be reported later.

DISCUSSION OF OXIDATION BEHAVIOR

During the Batch B fabrication campaign, both the US and the NIFS heat tubing experienced increases in total oxygen concentration that far exceeded the increase that occurred during the fabrication of the Batch A tubing from the US heat (Table 4). The magnitude of the oxygen increase was totally unexpected since examination of the processing records from Certified Metalcraft (CM) for Batch A revealed that the intermediate anneals had been carried out with reported vacuum levels in the 10^{-4} torr range. For Batch B the vacuum specification was raised to $>2 \times 10^{-5}$ torr and the records from Bodycote (BC) show that the measured vacuum levels ranged from 1.2×10^{-6} to 2.0×10^{-5} torr.

Table 4. Increase in interstitial concentrations (wppm)

Campaign	C	O	N
US BATCH A	220	390	10
US BATCH B	338	1414	82
NIFS BATCH B	331	1545	55
NIFS (JAPAN)	70	208	24

The increase in oxygen concentration during each one hour anneal at 1000°C is directly proportional to the impingement rate of oxygen atoms at the tube surface and to the SAV ratio of the tubing. The oxidation behavior of the two batches may be conveniently compared by plotting the incremental oxygen increase versus the SAV ratio for each anneal cycle. Although chemical analyses have not been completed on every archive sample taken, the increase in oxygen concentration for each stage can be estimated for Batch B from the smooth curve drawn through the chemical analysis data shown in Figs. 1 and 2. The oxygen increase data are tabulated in Table 5 together with the vacuum conditions reported by the vendor and plotted in Fig. 11. Deviations from proportionality occur because the vacuum conditions and hence the impingement rate of oxygen atoms vary from one anneal to the next; the error bars reflect the uncertainty in oxygen analysis.

Table 5: Estimated oxygen pick-up data for Batch B

Anneal No.	Wall (mm)	SAV (mm^{-1})	O Content (wppm)	O Increase (wppm)	Vacuum (10^{-6} torr)
4	2.85	0.70	375	20	5.1
5	2.13	0.94	400	25	4.0
6	1.52	1.3	450	50	2.6
7	1.22	1.6	525	75	2.8
8	0.99	2.0	625	100	1.2
9	0.81	2.5	760	135	3.8
10	0.64	3.2	950	190	7.2
11	0.48	4.1	1170	220	10.1
12	0.38	5.3	1425	255	12.1
13	0.31	6.6	1745	320	10.3

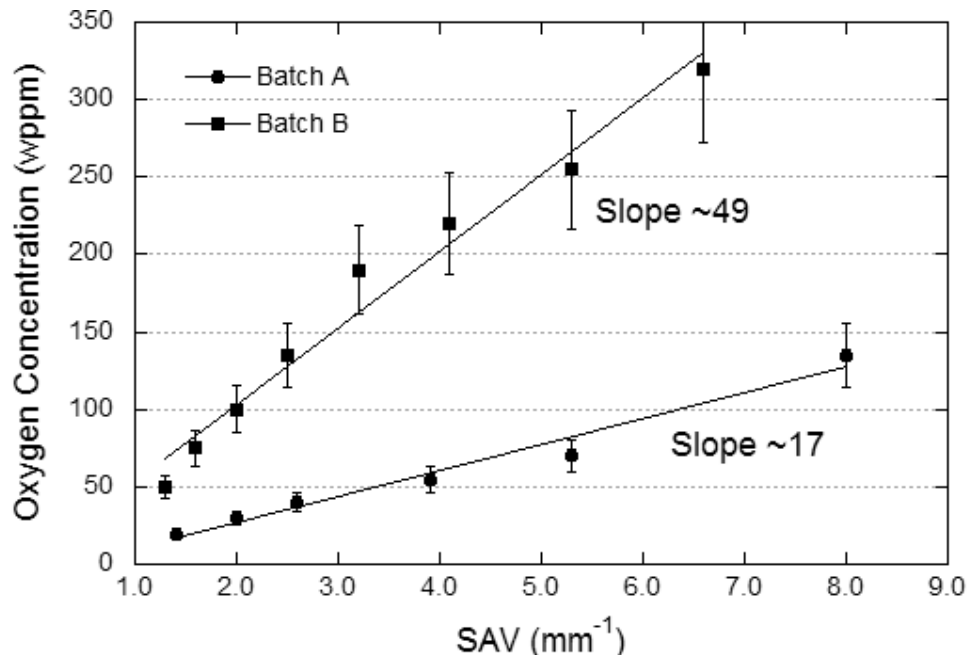


Figure 11. Linear curve fit to data. Error bars are 15% of the calculated value.

The only oxygen data available for Batch A are the initial and final analyses. The SAV ratios for the 10 cycles are plotted in Fig. 12 (The SAV ratio decreased during draw 9 which was a sinking operation to increase the final wall thickness). Superimposing the initial and final oxygen concentrations on a curve

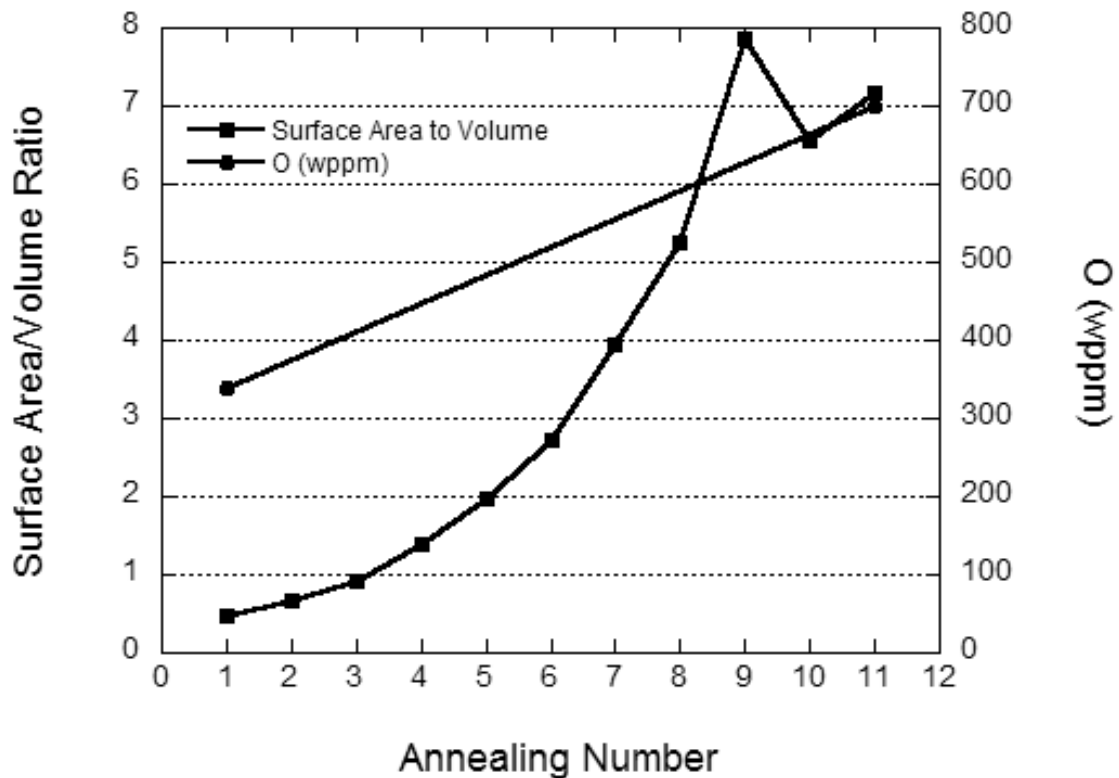


Figure 12. SAV ratio and O concentration versus annealing cycle for Batch A tubing (US Heat).

with the same shape as the SAV ratio curve allows us to estimate the incremental oxygen increase for each anneal; these incremental values are shown on Table 6 and plotted versus SAV ratio in Fig. 10. A comparison of the slopes of the two lines in Fig. 10 indicates that the increase in oxygen concentration for a given SAV ratio was a factor of 3-4 lower during the processing of Batch A than it was during the processing of Batch B.

Table 6 : Estimated oxygen pick-up data for Batch A

Anneal No.	Wall (mm)	SAV (mm^{-1})	O Content (wppm)	O Increase (wppm)
3	2.16	0.93	330	
4	1.45	1.4	350	20
5	1.02	2.0	380	30
6	0.77	2.6	420	40
7	0.51	3.9	475	55
8	0.38	5.3	545	70
9	0.25	8.0	680	135

The procedures followed together with the recorded heat treatment data from the two vendors were examined in an attempt to identify the origins of the factor of 3-4 difference in oxygen pick-up between the two batches. At least experimental 3 factors could be contributing the higher oxygen pick-up rates for Batch B, namely, a) differences in furnace geometry, vacuum measurement techniques and furnace leak

rates, b) differences in gettering methods and c) differences in the rate of attack and removal of surface layers during chemical cleaning.

The intermediate heat treatments for Batch A were carried out in a horizontal tube furnace ~60 cm in diameter with a volume of ~170 liters. On the other hand the Batch B heat treatments were carried out in a furnace measuring ~150 cm in diameter with a volume of ~2760 liters. The internal surface area of the BC furnace is a factor of x50 greater than that of the CM furnace. The large volume and surface area of the BC furnace coupled with a high pumping rate and a high leak rate could possibly result in higher partial pressures of oxygen and water vapor than indicated by the ion gauge readings. However information on leak rates is not available from either of the vendors. For the Batch B processing, Ta foil was substituted for the Ti wrap used during Batch A processing because of problems associated with the diffusion bonding of the Ti foil to the tube surface. Although Ti is somewhat more effective getter than Ta, it was considered that the difference was not sufficiently great to off-set the order-of-magnitude better vacuum measured in the BC furnace. During the Batch A processing the same Ti tent was used throughout whereas for Batch B, fresh Ta foil was used for each anneal.

For the Batch A processing, the acid cleaning stage immediately prior to vacuum heat treatment consisted of 5 minutes in a 30HNO₃-10HF-60H₂O solution; the original solution was used unchanged for the complete processing. For Batch B, because of concerns regarding pitting or grain boundary attack, the acid cleaning time was reduced to 30 seconds and the solution changed to 30HNO₃-20HF-50H₂O: again, the same solution was unchanged for all the cleaning stages. Because of the longer exposure time it is likely that surface layer removal by chemical etching after each draw cycle was greater during Batch A. However it is difficult to assess whether the rate of dissolution was aggressive enough to remove a sufficient depth of oxidized material to explain the measured differences in oxygen pick-up for the two batches. Tests carried out at ORNL with the latter solution indicate that a 3 minute immersion removes ~0.0005 in.

MODIFIED FABRICATION PROCEDURE; BATCH C

In an effort to produce a batch of tubing with a lower final oxygen concentration, the procedure used for Batch B was modified in several respects with the objective of lowering the oxygen pick-up rate by a factor of (3-4). Tube A1, which had been held back following anneal No. 8 was used as the starting material with the tube dimensions being 8.08mm OD with a 0.99mm wall and the oxygen concentration at 637wppm. Following a draw cycle of ~30% R/A, the tube was put through a sanding process to remove approximately 0.025 mm from the outside surface followed by the normal de-greasing operation and an extended chemical cleaning in the HNO₃/HF solution for 5 minutes. This resulted in a wall thickness of 0.71 mm (0.028 in) Chemical analysis at this stage showed that these surface treatments were effective in reducing the overall oxygen concentration from 637 wppm to 497 wppm. This tubing was then tented with an inner layer of fresh Ta foil and an outer layer of fresh Ti foil and annealed in the BTH furnace. The time at temperature was reduced from 1 hour to 30 minutes. To provide an additional measurement of the oxidation rate, a sample of the US heat in the form of a 0.5 mm thick sheet (S40) with an initial oxygen content of 366 wppm was also placed inside the Ta/Ti tent. The chemical analysis data from these operations are shown in Table 7.

Table7: Chemical analysis data for Batch C

Condition	I.D.	C (wppm)	O (wppm)	N (wppm)	O Change
Annealed Tube	A1	179	637	101	
30% RA; Sand/acid clean	C1	171	497	98	(140)
1000°C 30 min	C1-A	175	594	150	97
30%CW sheet	S40	135	366	97	
1000°C 30 min	S40-1	140	450	186	84

To assess the effectiveness of reducing the anneal time and introducing Ti in addition to the Ta wrap, the changes in oxygen content must be compared at the same thickness (SAV ratio). The increases in oxygen that occurred during the processing of Batch A and Batch B at the same SAV ratio as the Tube C1 sample were obtained from Figs. (q) and (s) and summarized in Table 8.

Table 8: Comparison of O pick-up for Batches B and C

I.D.	Thickness (mm)	SAV (mm ⁻¹)	O Increase (wppm)	Anneal Time (min)	Getter
C1-A	0.71	2.8	97	30	Ta + Ti
Batch B	0.71	2.8	145	60	Ta
Batch A	0.71	2.8	42	60	Ti

The combination of reduced time at temperature and adding Ti as a getter reduced the oxygen pick-up at a tube wall thickness of 0.71 mm from 145 to 97 wppm.. The experimental uncertainty in measuring change in oxygen concentration is approximately +/- 25 wppm. This magnitude of change in oxygen pick-up could be entirely accounted for by the factor of two reduction in annealing time and it is evident that the addition of a Ti getter has a minimal effect under the conditions pertaining to the BHT furnace. It is concluded that the use of the Ti getter during Batch A processing was not responsible for the observed lower oxygen pick-up rates. This experiment therefore indicated that the lower oxygen pick-up rates experienced during Batch A processing (60 min. anneals) are related to more favorable vacuum furnace geometry and leak rate conditions at CM in spite of the fact that the vacuum gauge readings were an order of magnitude higher than in the BHT furnace. To assess this possibility, a second experiment was carried out to compare directly, the oxygen pick-up in the two furnace systems.

The Tube C1-A was given a further draw cycle of 28.4% R/A, and then given the surface sanding treatment followed by the 5 min acid cleaning procedure. This resulted in a tube with a 6.42 mm OD and a wall thickness of 0.533 mm Two 55 cm long sections of this tubing were wrapped in both Ta and Ti and heat treated at the two vendors for 30 minutes at 1000°C with a request to maintain a vacuum of $>2 \times 10^{-5}$ torr. The furnace used at CM was the same furnace that was used for the processing of Batch A. The preliminary results of this comparison were surprising, but instructive. The tube that was annealed at CM was covered with a brownish oxide film whereas for the BC tube, the surface appearance was unchanged by the anneal at 1000°C. A coupon of the US heat sheet material (S40) was included and this also developed a surface oxide during the anneal at CM. Chemical analysis of these materials is not available at this time but the preliminary conclusion can be drawn that the vacuum gauge readings reported by the vendors (CM $\sim 10^{-4}$ torr; BC $< 2 \times 10^{-5}$ torr) are a reasonable indication of the different vacuum conditions at the tubing and that the partial pressure of oxygen is indeed much higher in the CM furnace used in the processing of Batch A tubing. It is concluded that the differences in furnace volume and surface area, leak rate etc. are not responsible for the higher oxygen pick-up rates in the Batch B annealing treatments carried out at BC.

It now seems highly probable that the differences in behavior between the two batches of tubing are related to differences in the mechanisms of oxidation of V-4Cr-4Ti when exposed to different partial pressures of oxygen at 1000°C. A possible explanation of the observed behavior may be found in the work of Pint and DiStefano [6] who studied the kinetics of oxidation of the US heat of V-4Cr-4Ti at 600-700°C under partial pressures of oxygen in the range 10^{-3} - 10^{-6} Pa. It was found that at very low oxygen partial pressures, oxidation is limited by a surface reaction such as oxygen absorption and the oxidation kinetics are linear. However at higher oxygen partial pressures a surface oxide may form and oxygen uptake is limited by diffusion through the surface oxide and under these conditions the kinetics take a linear-parabolic form. The observation of a visible oxide film during the 1000°C anneal in the CM furnace and not in the BC furnace indicates that we are in two different oxidation regimes due to the differences in oxygen partial pressure. A possible scenario is that during the Batch A annealing at CM, oxygen pick-up in the bulk of the tubing was limited by the formation of a temporarily protective oxide layer. This oxide layer remained on the tubing during the next draw cycle and could possibly have contributed to the fairly

high incidence of surface cracking on the OD and ID of the Batch A tubing. The subsequent 5 minute acid cleaning could well have been sufficient to remove the oxide layer and therefore a major fraction of the oxygen picked-up during the anneal. On the other hand, during the annealing treatments in the better vacuum conditions prevailing in the BC furnace, no protective layer was formed and the oxygen up-take was correspondingly much higher. Very little of the oxygen was removed during the acid cleaning because a) the oxygen was not concentrated in a surface oxide and b) the acid cleaning time was only 30 seconds duration.

FUTURE WORK

Further investigation of tubing samples taken from these experiments is in progress including the effectiveness of the acid cleaning process in lowering overall oxygen concentration. Oxidation rates will be estimated based on the weight gains calculated from the oxygen analyses and compared with empirical oxidation model [6]. Once the reasons for the high oxygen pick-up rates during the Batch B processing are understood, it should be possible to develop a procedure that limits oxygen pick-up during processing and proceed to the preparation of a new batch of creep tubing for both heats utilizing the 8.08mm OD tubing that was held back following the eighth annealing cycle.

REFERENCES

1. H. Tsai, M.C. Billone, R.V. Strain, and D.I. Smith; Fusion Materials Semi-annual Progress Report, DOE/ER-0313/23, December 1997, p.149.
2. M.L. Grossbeck, R.J. Kurtz, L.T. Gibson, and M.J. Gardner; Fusion Semi-annual Progress Report, DOE/ER-0313/32, June 2002, p. 6.
3. H. Tsai, M.C. Billone, T.S. Bray and D.L. Smith; Fusion Semi-annual Progress Report, DOE/ER-0313/27, December 1999, p. 65.
4. T. Nagasaka, T. Muroga, T. Likbo, "Development of Tubing Technique for High-Purity Low Activation Vanadium Alloys," ANS Winter Meeting, Washington DC, Nov. 2002, (to be published).
5. A.F. Rowcliffe, W.R. Johnson and D.T. Hoelzer; Fusion Materials Semi-annual Progress Report, DOE/ER-0313/33 , December 2002, p. 7.
6. B.A. Pint and J.R. DiStefano, "Oxygen Embrittlement of Vanadium Alloys With and Without Surface Oxide Formation," J. Nuclear Materials, 307-311, 2002, p. 560.